Molecular sorting on a fluctuating membrane

D. Andreghetti [1,2], L. Dall'Asta[1,2,3,4], A. Gamba[1,2,3,⋆], I. Kolokolov[5,6] and V. Lebedev[5,6]

1 Institute of Condensed Matter Physics and Complex Systems, Department of Applied Science and Technology, Politecnico di Torino, Corso Duca degli Abruzzi 24, 10129 Torino, Italy
2 Istituto Nazionale di Fisica Nucleare (INFN), Italy
3 Italian Institute for Genomic Medicine c/o Candiolo Cancer Institute, Fondazione del Piemonte per l'Oncologia (FPO), Istituto di Ricovero e Cura a Carattere Scientifico (IRCCS), Candiolo, 10060 Torino, Italy
4 Collegio Carlo Alberto, Via Real Collegio 30, 10024 Moncalieri, Italy
5 L.D. Landau Institute for Theoretical Physics, 142432, Moscow Region, Chernogolovka, Ak. Semenova, 1-A, Russia
6 National Research University Higher School of Economics, 101000, Myasnitskaya 20, Moscow, Russia

⋆ andrea.gamba@polito.it

Abstract

Molecular sorting in biological membranes is essential for proper cellular function. It also plays a crucial role in the budding of enveloped viruses from host cells. We recently proposed that this process is driven by phase separation, where the formation and growth of sorting domains depend primarily on short-range intermolecular interactions. In addition to these, Casimir-like forces—arising from entropic effects in fluctuating membranes and acting on longer ranges—may also play a significant role in the molecular distillation process. Here, using a combination of theoretical analysis and numerical simulations, we explore how these forces contribute to sorting, particularly in the biologically relevant regime where short-range intermolecular interactions are weak. Our results show that Casimir-like forces enhance molecular distillation by reducing the critical radius for the formation of new sorting domains and facilitating the capture of molecules within these domains. We identify the relative rigidity of the membrane and supermolecular domains as a key parameter controlling molecular sorting efficiency, offering new insights into the physical principles underlying molecular sorting in biological systems.

Received Date
Accepted Date
Published Date

Contents

1 Introduction 2
2 Phenomenological Theory 3
3 Numerical results 6

4 Conclusions 8

A Interaction of a molecule with a domain 9

B Simulation protocol 11

References 13

1 Introduction

Molecular sorting is a vital process in eukaryotic cells, where proteins and other biomolecules are sorted and encapsulated into lipid vesicles for targeted transport to specific subcellular locations. This distillation process occurs on lipid membranes, such as the plasma membrane [1], endosomes, the Golgi apparatus [2], and the endoplasmic reticulum [3], where biomolecules can bind and diffuse laterally. Due to a variety of direct and indirect interactions, these molecules aggregate into domains with distinct chemical compositions. These domains can induce membrane bending and fission [4–7], ultimately forming separated submicron lipid vesicles that are transported to their designated subcellular sites by molecular motors. In this way, lipid membranes act as natural molecular distillers, promoting intracellular order and compartmentalization and counteracting the homogenizing effects of diffusion. Disruption of molecular sorting in living cells is implicated in severe pathologies, including cancer [8, 9]. On the other end of the spectrum, analogous molecular sorting processes are exploited by enveloped viruses, such as HIV, SARS-CoV, and influenza, for their assembly and budding from host cells [10–13], further underscoring the practical relevance of understanding the physical mechanisms of molecular sorting.

We have recently proposed a simple model of molecular sorting as a phase-separation process. In this context, the efficiency of sorting is found to be optimal at intermediate values of intermolecular attraction forces [14–16]. This theoretical prediction is consistent with experiments on endocytic sorting in living cells under near-physiological conditions [14], and with measurements performed on photoactivated systems, where the strength of intermolecular attraction can be directly controlled [17]. The interpretation of molecular sorting as a phase-separation process is also coherent with the observation that sorting domains in living cells exhibit a critical size: only supercritical (“productive") domains evolve into lipid vesicles that are extracted from the membrane, while subcritical (“unproductive") domains are rapidly dissolved [15, 18].

Phase separation is emerging as one of the main ordering processes in living cells [19–21], and various mechanisms have been proposed as its drivers. Among them, weakly polar electrostatic interactions between disordered regions of proteins [22], active processes, as in diffusion-limited phase separation, mass-conserved reaction-diffusion systems and active emulsions [23–29], and segregating kinetic effects [30]. On the other hand, it has long been established that protein inclusions in lipid membranes are subject to Casimir-like interactions [31, 32, 49], a significant class of entropic interactions. However, their role in molecular sorting remains unexplored. These interactions arise from the increased rigidity of the membrane in the presence of embedded protein inclusions, which restricts membrane fluctuations and generates entropic attractive forces. It is known that proteins and lipids involved in the formation of sorting domains increase local membrane rigidity by a factor of 10 to 30 compared to the surrounding membrane [33–35]. Here, we investigate the role of these Casimir-like inter-

actions in molecular sorting and find that they can significantly enhance the molecular sorting process, especially within the biologically relevant regime of weak short-range interactions.

2 Phenomenological Theory

Building on our previous work, we investigate the role of the lipid membrane as a distiller of molecular species [14–16]. In this scenario, molecules are randomly inserted into the membrane, diffuse laterally, and aggregate into sorting domains due to short-range attractive forces. The sorting domains grow by adsorbing molecules from the surrounding "gas" of freely diffusing molecules. Domains of size R larger than a critical value R_c grow irreversibly through the absorption of single molecules diffusing towards them [15, 36, 37]. The growth rate is determined by the net flux Φ of molecules towards a domain, which in turn is proportional to the molecular density difference $\Delta n = n_L - n_R$ between distant regions and regions adjacent to the domain boundaries [14]. Domains that reach a characteristic size R_E are ultimately removed from the membrane through the formation of small, separate lipid vesicles [14].

Of particular interest is the stationary out-of-equilibrium regime, where molecular insertion and extraction processes are balanced. This balance can be described by the equation

$$\phi = N_d \Phi, \tag{1}$$

where ϕ is the flux density of molecules being inserted into the membrane, N_d is the density of supercritical domains, and Φ is the average flux of the molecules into a domain. In this regime, unlike in the classical Lifshitz-Slezov scenario [36, 37], the flux-driving jump Δn in molecular density is kept finite by the continuous influx ϕ of molecules into the membrane.

We have shown in Ref. [14] that an optimal sorting regime is achieved for an intermediate strength of short-range attractive forces. When the tendency to aggregate is too strong, a proliferation of slowly growing sorting domains occurs, leading to molecular crowding and decreased sorting efficiency [14, 16]. In the optimal sorting regime, there exists a specific density N_d of sorting domains, resulting in minimal average molecular density [14]. For absorbing domains, the average residence time T of a molecule of linear size a in the membrane system is the sum of the average time T_f required for the molecule to reach a sorting domain by free diffusion and be absorbed, and the average time T_d spent inside the domain until the extraction event. The two contributions can be estimated as [14]

$$T_f \sim \frac{1}{DN_d}, \quad T_d \sim \frac{(R_E/a)^2}{\phi} N_d,$$

where D is the molecular diffusion coefficient. The sum $T = T_f + T_d$ has a minimum for

$$N_{d,opt} \sim \frac{a}{R_E}\sqrt{\frac{\phi}{D}}. \tag{2}$$

The actual density N_d is a function of the microscopic properties of the system that control the nucleation and growth of domains in the stationary state, but irrespective of the combination of these microscopic quantities, the optimal residence time of molecules on the membrane has the value determined by Eq. (2).

To account for the role of membrane fluctuations in the molecular sorting process described above, we recall that the equilibrium thermal fluctuations of an elastic membrane are described by the Helfrich Hamiltonian,

$$\mathcal{H} = \int dS \left[\frac{\kappa}{2}\left(\frac{1}{R_1} + \frac{1}{R_2}\right)^2 + \frac{\bar{\kappa}}{R_1 R_2} \right], \tag{3}$$

where the integral runs over the membrane surface, dS is the area element, R_1, R_2 are local principal curvature radii, and $\kappa, \bar{\kappa}$ are the bending rigidities associated with the mean and Gaussian curvatures, respectively [38–40]. As argued in Refs. [41–43], for biological membranes, $\bar{\kappa}$ is close to $-\kappa$. While our theory remains valid for any relation between κ and $\bar{\kappa}$, for simplicity we will assume that $\bar{\kappa} = -\kappa$ in the numerical computations presented in the following section. In the presence of protein inclusions, the rigidity of the membrane becomes spatially non-uniform. Here, we assume that $\kappa(\mathbf{r}) = \kappa_0$ for the bulk membrane, and $\kappa(\mathbf{r}) = \kappa_1$ in the regions occupied by the molecules. A surface-tension contribution to the energy could also be included, but it is assumed to be negligible and will not be considered here.

We further assume that the diffusive dynamics of protein inclusions is slower than the fluctuational dynamics of the underlying membrane, i.e., $\tau_{\rm diff} \gg \tau_{\rm rel}$, with $\tau_{\rm diff}$ the characteristic diffusion time and $\tau_{\rm rel}$ the characteristic membrane relaxation time. This is motivated by the following estimates. The characteristic time for lateral diffusion can be estimated as $\tau_{\rm diff} \sim \lambda^2/D$, where λ is the characteristic scale of the problem. Assuming that the viscosity η of the cytosol is the primary source of dissipation, the characteristic relaxation time of the membrane dynamics is $\tau_{\rm rel} \sim \eta\lambda^3/\kappa$ [44]. Since the ratio $\tau_{\rm rel}/\tau_{\rm diff}$ increases as λ grows, one should check whether the inequality $\tau_{\rm diff} \gg \tau_{\rm rel}$ holds for the largest characteristic scale, that is, for the size of the membrane. Considering membranes with sizes $\lambda = 100 - 500\,\mathrm{nm}$, taking the viscosity $\eta \sim 5 \cdot 10^{-3}\mathrm{Pa}\cdot\mathrm{s}$ and the lateral diffusivity D of proteins in the range $1 - 10\ \mu\mathrm{m}^2/\mathrm{s}$ [45, 46], one finds that the ratio $\tau_{\rm diff}/\tau_{\rm rel}$ spans the values $1 - 10^2$, suggesting that the dynamics of membrane fluctuations in living cells is faster than lateral particle diffusion [44, 47, 48].

Membrane fluctuations are known to induce long-range effective interactions between inclusions within the membrane. These interactions can be conveniently studied in the weak fluctuation regime, where quantitative analyses can be performed [31, 49–53]. It is of particular interest to investigate how these forces interplay with short-range forces to facilitate the absorption of neighboring molecules by sorting domains.

Analytic expressions for membrane-mediated forces can be derived in various limit cases. We are interested here in the interaction of a circular domain of size R with a molecule of linear size a situated at a distance x from it. Approximating the domain boundary in zeroth order as an infinite straight wall under the condition $R \gg x \gg a$, the effective potential energy of the membrane-mediated interactions is given by:

$$U(x) \;=\; -A\,k_{\rm B}T\,\frac{a^2}{x^2} \tag{4}$$

where A is a dimensionless, increasing function of the relative rigidity $\alpha = \kappa_1/\kappa_0$ (see Appendix A). Eq. (4) implies that $U \sim A k_{\rm B}T$ near the surface of a domain. On the other hand, the interaction potential between two inclusions mediated by the membrane fluctuations decays as r^{-4} for distances r much larger than their sizes [31].

The process of lateral diffusion of a molecule situated near a circular sorting domain can be described by the biased Brownian motion

$$\dot{\mathbf{r}} \;=\; -\beta D \nabla U(\mathbf{r}) + \boldsymbol{\xi},$$

where $\beta = (k_{\rm B}T)^{-1}$. According to the fluctuation-dissipation theorem, the noise term $\boldsymbol{\xi}$ satisfies

$$\begin{aligned} \langle \xi_i(t) \rangle &= 0 \\ \langle \xi_i(t)\xi_j(t) \rangle &= 2\,D\,\delta_{ij}\,\delta(t-t'). \end{aligned}$$

It is worth observing here that in the limit of weak fluctuations, geometric effects caused by the projection of the molecule's path can be neglected [54, 55]. Moreover, deviations of the

domain shape from circularity produce rapidly decaying higher multipole contributions that may be neglected in the main approximation.

The time-dependent density profile of a population of such diffusing molecules around a domain obeys the following diffusion equation

$$\partial_t n(\mathbf{r},t) \quad = \quad \nabla\cdot[D(\nabla+\beta\nabla U)n(\mathbf{r},t)] \tag{5}$$

where n is the two-dimensional molecular density. To study the growth of the domain, one can consider an isotropic, time-independent solution to Eq. (5). The assumption of isotropy is justified by the circular shape of the domain, while the approximate time independence is supported by the slow nature of the diffusion process. Consequently, n and U depend only on the distance r from the center of the domain. The explicit expression for $n(r)$ is given by:

$$n(r) \quad = \quad n(R)\exp[\beta U(R)-\beta U(r)]+\frac{\Phi}{2\pi D}\int_R^r \frac{\mathrm{d}\rho}{\rho}\exp[\beta U(\rho)-\beta U(r)], \tag{6}$$

where R is the radius of the domain and $n(R)$ is the molecular density near the domain boundary. The potential U, induced by membrane fluctuations, is of the order of $k_\mathrm{B}T$ when $r\sim R$ and tends to zero as r grows (see Appendix A). Thus, for $r\gg R$, the solution (6) reduces to

$$n(r) = n(R)\,\mathrm{e}^{\beta U(R)}+\frac{\Phi}{2\pi D}\ln\frac{r}{\tilde{R}}, \tag{7}$$

where $\tilde{R}\sim R$. For the attractive potential induced by membrane fluctuations, $U<0$, $\tilde{R}>R$ and $\tilde{R}-R\sim R$. The factor $\mathrm{e}^{\beta U(R)}$ in Eq. (7) is of order unity.

The density of molecules near the domain boundary is determined by the dynamic equilibrium of association and dissociation processes and can be expressed as

$$n(R) = n_0(1+R_\star/R), \tag{8}$$

where n_0 is the equilibrium density near a straight boundary, and the R-dependent correction accounts for the effect of linear tension. This correction is directly related to the curvature of the domain boundary. The length $R_\star$ in Eq. (8) can be estimated to be of the order of a few molecular radii. Expression (8) allows to determine the critical radius R_c: by definition, a domain with radius R_c remains static, since the flux Φ for such a domain is zero. Substituting $\Phi=0$ and $n(r)=n_L$ (where n_L is the concentration of the molecules far from the domains) into Eq. (7) yields:

$$\frac{R_\star}{R_\mathrm{c}} \quad = \quad \frac{n_L}{n_0}\,\mathrm{e}^{-\beta U}-1. \tag{9}$$

Since $\exp(-\beta U)>1$ for the attractive potential, we conclude from Eq. (9) that membrane-induced attraction reduces the critical radius. For domains larger than R_c, the correction related to the linear tension can be neglected, resulting in $n(R)\to n_0$. Consequently, we find from Eq. (7):

$$n_L - n_0\,\mathrm{e}^{\beta U} = \frac{\Phi}{2\pi D}\ln\frac{L}{\tilde{R}}, \tag{10}$$

where L is a distance of the order of the separation between the domains. Since $\exp(\beta U)<1$ for the attractive potential, we conclude from Eq. (10) that membrane-mediated attraction enhances the effectiveness of the clustering process, resulting in an increased flux Φ.

The above relations show how forces mediated by membrane fluctuations affect the sorting process. Let us examine the effect of increasing membrane-mediated attraction (which can

be directly adjusted in numerical simulations by varying the relative rigidity $\alpha = \kappa_1/\kappa_0$). As membrane-mediated attraction increases, the critical radius R_c of the domains decreases, leading to a higher rate of production of germs of new sorting domains and, consequently, an increased overall density N_d of sorting domains [37]. However, according to the balance relation (1), this should concomitantly result in a lower Φ and, in accordance with Eq. (10), a lower n_L, which in turn reduces the rate of new domain generation. Between these two opposing effects, the first is expected to dominate due to the high sensitivity of the process of germ generation to the critical radius R_c [37]. Below, we present results from numerical simulations that confirm this expectation.

It is worth observing here that in the stationary state, the density N_d of sorting domains is self-consistently determined through the stationarity condition $dN_d/dt = \phi/N_E$, where N_E is the average number of molecules removed during an extraction event, since the rate of formation of new domains dN_d/dt is in average equal to the rate of extraction events. [14, 15]. Starting from the regime of weak short-range interactions, the optimal density of sorting domains $N_{d,\mathrm{opt}}$ determined by Eq. (2) can be reached either by increasing the short-range interaction strength, or by reducing the critical radius by means of increased molecular rigidities κ_1. Conversely, to increased molecular rigidities should correspond lower values of the optimal short-range interaction strength.

3 Numerical results

To validate our theoretical predictions, we implemented a numerical scheme that generalizes the lattice-gas model of molecular sorting introduced in Ref. [14]. This scheme shares several features with the approach used in Ref. [56] to investigate the phase separation of rigid inclusions in fluid membranes close to thermodynamic equilibrium, although we are studying here an out-of-equilibrium state. We consider a fluctuating membrane described by a discretized version of Helfrich Hamiltonian, on which inserted molecules laterally diffuse and aggregate. The system is driven out of equilibrium by an incoming flux of molecules, which are randomly attached at empty membrane sites with a rate ϕ per unit area, and is maintained in a statistical stationary state by the instantaneous removal of connected molecular domains that reach the threshold number of molecules N_E. Consistently with our theoretical approach, simulations are performed in the adiabatic regime.

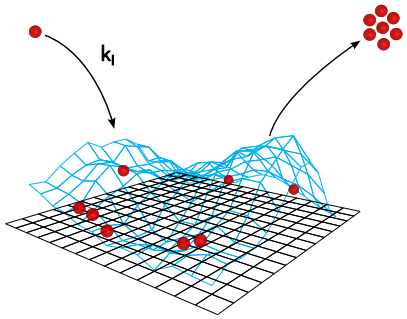

Figure 1: Schematic representation of the discrete model of molecular sorting on a fluctuating membrane. The membrane (in blue) is described by its height relative to a reference plane (in black). Rigid molecules are inserted into vacant sites at a rate k_I, and connected domains containing more molecules than the threshold size N_E are extracted. The amplitude of membrane fluctuations is here amplified for the sake of clarity.

In our numerical scheme, the membrane configuration is described by the height u_i of its points relative to a reference plane, which is discretized into a square lattice of $L \times L$ sites, see Fig. 1. To avoid boundary effects, periodic boundaries conditions are applied. Each site of the lattice can be occupied by at most one molecule. An occupation number $n_i \in \{0,1\}$ is associated to each site i. Sites with $n_i = 0$ have the bending rigidity κ_0, while sites with $n_i = 1$ have the rigidity κ_1. The corresponding Gaussian rigidities are assumed to be equal to $-\kappa_0$ and $-\kappa_1$, respectively. To account for the short-range attractive force between membrane inclusions we add to the discretized Helfrich energy of the membrane the nearest-neighbor interaction energy

$$H_{\rm incl} = -\frac{W}{2}\sum_{\langle i,j\rangle} n_i n_j \tag{11}$$

Membrane configurations are sampled using a Monte Carlo algorithm. After each Monte Carlo sweep (MCS), steps involving molecule insertion, diffusion, and the extraction of domains of size $\geq N_{\rm E}$ are performed. One MCS is taken as the time unit. The rate of molecule insertion per empty site is denoted by $k_{\rm I}$. The diffusion rate $k_{\rm D}$ of free molecules is measured as the ratio of accepted diffusive jumps during one MCS (see Appendix B for additional details). Simulations are performed with the realistic parameter values $\kappa_0 = 10\, k_{\rm B}T$, $N_{\rm E} = 25$ [14–16,57,58], while k_I and k_D are kept much smaller than 1 in inverse MCS units, to ensure proper sampling of membrane configurations within the adiabatic regime.

The average density $\bar{\rho}$ of molecules in the stationary state satisfies the relation $\bar{\rho} = \phi\, T$, where T is the average time a particle spends on the membrane before being extracted, and $\phi = k_{\rm I}(1-\rho)$ is the flux of incoming particles per site, if lengths are measured in units of the lattice spacing [14,59]. Therefore, in the statistically stationary state established at fixed ϕ, the average density $\bar{\rho}$ is a measure of the efficiency of the sorting process [14].

We investigated the behavior of the density $\bar{\rho}$ as a function of the short-range interaction W and molecular rigidity κ_1. In Fig. 2, the resulting stationary densities are plotted as functions

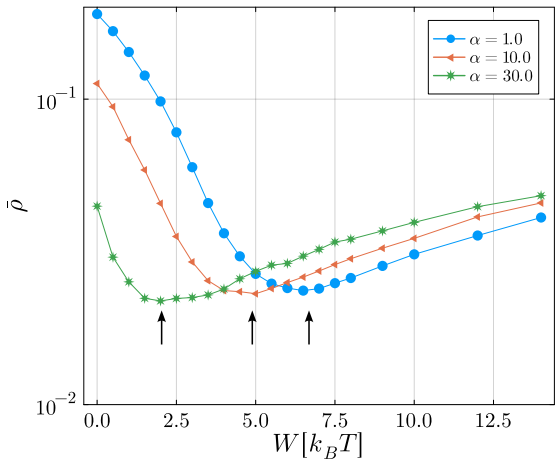

Figure 2: Average density $\bar{\rho}$ in the stationary state as a function of the short-range interaction strength W. The different curves correspond to different values of $\alpha = \kappa_1/\kappa_0$. In these simulations, the dimensionless flux is $\phi/k_{\rm D} = 10^{-5}$. The optimal sorting region depends on both the short-range interaction and the rigidity of the biomolecules involved. To larger values of the relative molecular rigidity α there correspond lower values of the optimal short-range interaction strength $W_{\rm opt}$ (arrows).

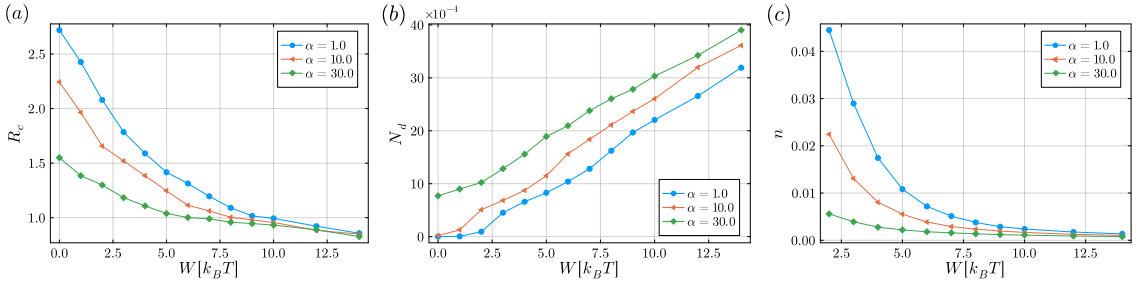

Figure 3: Characterization of the sorting process in the statistically steady state in terms of three key observables, measured from numerical simulations as functions of the short-range interaction strength W, for varying relative rigidities $\alpha = \kappa_1/\kappa_0$: (a) the critical radius R_c (estimated using the method described in Ref. [15]); (b) the number density N_d of supercritical domains; and (c) the average density of isolated molecules $\bar{n}$. Due to the logarithmic profile of the molecular density around sorting domains, the average density $\bar{n}$ is close to n_L.

of the short-range interaction strength W for the fixed dimensionless flux $\phi/k_D = 10^{-5}$ (see Appendix B), with varying $\alpha = \kappa_1/\kappa_0$.

These numerical results confirm the theoretical prediction that membrane-mediated interactions strongly influence the molecular sorting process, and that the optimal short-range interaction strength W_{opt} decreases as the intensity of membrane-mediated interactions increases, thus enhancing sorting efficiency in the biologically relevant regime of weak short-range interactions.

To further validate the present theoretical scenario, we measured the critical size R_c, the number density of sorting domains N_d, and the average density of isolated molecules $\bar{n}$ (which is approximately the same as n_L) for varying values of W and α (Fig. 3). Consistent with the theoretical predictions, the critical size R_c decreases monotonically with both increasing W and α (Fig. 3a), resulting in a higher sorting domain density N_d (Fig. 3b). This confirms that, in the presence of membrane-mediated interactions, the optimal sorting-domain density $N_{d,opt}$ is achieved at lower short-range interaction strengths W. As predicted, the increase in sorting-domain density is reflected in a corresponding decrease in the average density of isolated molecules $\bar{n}$ (Fig. 3c).

4 Conclusions

The lipid membranes of endosomes, the Golgi apparatus, the endoplasmic reticulum, and the plasma membrane play a fundamental role in sorting and distilling vital molecular factors, acting as a natural realization of Szilard's model of classical nucleation theory [37]. These delicate structures are inherently subject to thermally induced fluctuations. Previous studies have shown that such fluctuations significantly contribute to the phase separation of rigid membrane inclusions close to thermodynamic equilibrium [56]. Our analysis extends these findings to the out-of-equilibrium scenario of molecular sorting, demonstrating that membrane-mediated interactions can strongly enhance the molecular distillation of rigid inclusions, particularly, in the biologically relevant regimes where short-range intermolecular attractive forces are relatively weak. Our analysis suggests that thanks to membrane-mediated interactions, rigid biomolecules can be sorted with high efficiency, despite their low-affinity interactions. Notably, this effect, potentially crucial for biological systems, is observed in our numerical simulations well below the threshold where phase separation occurs close to equilibrium [56]. This sug-

gests an important distinction between classical quasi-equilibrium phase separation processes and the role phase separation plays in out-of-equilibrium biological systems.

Molecular inclusions interact with the surrounding membrane due to both their rigidity and, possibly, non-zero intrinsic curvature [31,60] In this study, we have focused on the impact of rigidity on the molecular sorting process. In future work, we plan to investigate the complex interplay between rigidity and intrinsic curvature.

Our findings suggest that a key parameter controlling molecular sorting efficiency is the relative rigidity of the membrane and supermolecular domains, and that higher efficiency is achieved at intermediate values of this relative rigidity. These predictions may inspire future experimental investigations in real biological cells or in artificially prepared membranes.

Acknowledgements

AG would like to thank Guido Serini for many fruitful discussions.

Funding information Numerical calculations have been made possible through a CINECA-INFN agreement providing access to computational resources at CINECA.

A Interaction of a molecule with a domain

In this section, we analyze the Casimir interaction between a circular domain of radius R and a single molecule of radius $a \ll R$, positioned at a distance $x \gg a$ from it. We will calculate the interaction potential between the molecule and the domain.

In the absence of overhangs, the membrane can be parameterized in the Monge gauge [61], where each point on the membrane is defined by its displacement $u(\mathbf{r}) = u(x,y)$ in the direction perpendicular to a reference plane $\mathcal{S}$. To second order in u, the Helfrich Hamiltonian, which provides the elastic energy of the deformed membrane, reads

$$\mathcal{H} = \int_{\mathcal{S}} \mathrm{d}x\,\mathrm{d}y\,\left\{\frac{\kappa}{2}(\nabla^2 u)^2 + \bar{\kappa}[\partial_x^2 u\,\partial_y^2 u - (\partial_x\partial_y u)^2]\right\}, \tag{A.1}$$

Here κ and $\bar{\kappa}$ are bending and Gaussian rigidities, determined by an internal structure of the membrane. A surface-tension contribution to the energy could also be included, but it is assumed to be negligible and will not be taken into account.

Here we consider the interaction of a single molecule with a circular domain of molecules inserted into the membrane. When the molecule is positioned at the point $\mathbf{r} = (x,y)$, the interaction potential of the molecule with the domain is

$$\begin{aligned} U \;=\; & B(\partial_x^2\partial_{x'}^2\mathcal{G}|_{x=x',y=y'} + 2\partial_x^2\partial_{y'}^2\mathcal{G}|_{x=x',y=y'} + \partial_y^2\partial_{y'}^2\mathcal{G}|_{x=x',y=y'}) \\ & + D(\partial_x^2\partial_{y'}^2\mathcal{G}|_{x=x',y=y'} - \partial_x\partial_y\partial_{x'}\partial_{y'}\mathcal{G}|_{x=x',y=y'}) \end{aligned} \tag{A.2}$$

where $\mathcal{G}(\mathbf{r},\mathbf{r}')$ is the contribution to the pair correlation function $\langle u(\mathbf{r})u(\mathbf{r}')\rangle$ from the membrane displacement induced by the domain. The factors B, D in Eq. (A.2) are introduced via the phenomenological coupling energy of the molecule with the membrane, when the former is treated as a point-like object:

$$\delta\mathcal{H} = B(\nabla^2 u)^2 + D[\partial_x^2 u\partial_y^2 u - (\partial_x\partial_y u)^2] \tag{A.3}$$

where the derivatives are evaluated at the position of the molecule. This expression is valid for fluctuations of u on scales much larger than a. The factors B and D are functions of the

rigidity and size of the molecule. We will make use of the fact that their expression for a disc of radius a and rigidity $\kappa = \kappa_1, \bar{\kappa} = -\kappa_1$, inserted in a membrane of rigidity $\kappa = \kappa_0, \bar{\kappa} = -\kappa_0$ is [52, 62]:

$$\begin{aligned} B &= \pi a^2 \kappa_0 (\kappa_1 - \kappa_0)\left(\frac{1}{(\kappa_1+\kappa_0)} + \frac{1}{\kappa_1+3\kappa_0}\right) \\ D &= -\pi a^2 \frac{4(\kappa_1-\kappa_0)\kappa_0}{\kappa_1+3\kappa_0}. \end{aligned} \tag{A.4}$$

If the separation between the molecule and the domain boundary is much smaller than the domain size R, the boundary can be approximated as a straight line. Therefore, we assume that the domain occupies the half-plane $x < 0$. We also consider that the domain and the bulk membrane have different bending and Gaussian rigidities, $\kappa_1, \bar{\kappa}_1$ and $\kappa_0, \bar{\kappa}_0$. respectively. The Hamiltonian of the system is then given by

$$\begin{aligned} \mathcal{H} = &\int_{\mathcal{D}_1} dx\, dy\, \left\{\frac{\kappa_1}{2}(\nabla^2 u)^2 + \bar{\kappa}_1[\partial_x^2 u \partial_y^2 u - (\partial_x\partial_y u)^2]\right\} \\ &+ \int_{\mathcal{D}_2} dx\, dy\, \left\{\frac{\kappa_0}{2}(\nabla^2 u)^2 + \bar{\kappa}_0[\partial_x^2 u \partial_y^2 u - (\partial_x\partial_y u)^2]\right\} \end{aligned} \tag{A.5}$$

where $\mathcal{D}_1$ is the left half-plane ($x < 0$) and $\mathcal{D}_2$ is the right half-plane ($x > 0$).

Using linear response theory, we can derive an equation for the pair correlation function $G = \langle u(\mathbf{r})u(\mathbf{r}')\rangle$, entering Eq. (A.2). It is important to note here that, due to the system's homogeneity in the y direction and its invariance under reflection $y \to -y$, G is a function of $|y - y'|$. The resulting equations read

$$\begin{aligned} \nabla^4 G &= \frac{k_B T}{\kappa_1}\delta(x-x')\delta(y-y') \qquad x < 0 \\ \nabla^4 G &= \frac{k_B T}{\kappa_0}\delta(x-x')\delta(y-y') \qquad x > 0 \end{aligned} \tag{A.6}$$

with boundary conditions

$$\begin{aligned} \partial_x(\kappa_1\nabla^2 - \bar{\kappa}_1\partial_y^2)G|_{x=0^-} &= \partial_x(\kappa_0\nabla^2 - \bar{\kappa}_0\partial_y^2)G|_{x=0^+} \\ (\kappa_1\nabla^2 + \bar{\kappa}_1\partial_y^2)G|_{x=0^-} &= (\kappa_0\nabla^2 + \bar{\kappa}_0\partial_y^2)G|_{x=0^+} \end{aligned} \tag{A.7}$$

Observe that, due to the inhomogeneity of the Gaussian rigidity, the topological term involving Gaussian curvature in the Hamiltonian cannot be neglected. This term contributes to the boundary conditions (A.7) for the correlation function.

Due to translation invariance along the y direction, it is convenient to make use of the Fourier transform

$$\hat{G}(x, x', q) = \int_{-\infty}^{+\infty} \mathrm{d}y\, \exp[iq(y-y')]G(x, x', y-y'),$$

which is an even function of q. The solutions to Eqs. (A.6) and (A.7) for $q > 0$ are

$$\hat{G}(x, x', q) = (A_0 + A_1 x)e^{qx} + \frac{k_B T}{4q^3\kappa_1}(1 + q|x-x'|)e^{-q|x-x'|}$$

for $x < 0$, and

$$\hat{G}(x, x', q) = (B_0 + B_1 x)e^{-qx} + \frac{k_B T}{4q^3\kappa_0}(1 + q|x-x'|)e^{-q|x-x'|}$$

for $x > 0$. The factors A_0, A_1, B_0, B_1 must be determined from the continuity of $\hat{G}$ and its derivative $\partial_x \hat{G}$ at $x = 0$ and from the boundary conditions (A.7), where $\partial_r^2 \to -q^2$, $\nabla^2 \to \partial_x^2 - q^2$. Assuming $\bar{\kappa}_0 = -\kappa_0$ and $\bar{\kappa}_1 = -\kappa_1$, the correlation function for $x, x' > 0$ is

$$\hat{G}(x,x',q) = \frac{k_B T}{4q^3\kappa_0}\Bigg[(1+q|x-x'|)e^{-q|x-x'|} - \frac{e^{-q(x+x')}(\kappa_1-\kappa_0)((3\kappa_1+\kappa_0)q(x+x'+2qxx')+3\kappa_1+5\kappa_0)}{(3\kappa_1+\kappa_0)(\kappa_1+3\kappa_0)}\Bigg]. \quad \text{(A.8)}$$

The second term in the square brackets determines the contribution $\mathcal{G}$ to the correlation function induced by the domain.

In accordance with Eqs. (A.2,A.4,A.8) the interaction energy of the molecule with the domain is

$$U(x) = -A k_B T \frac{a^2}{x^2} \quad \text{(A.9)}$$

where, letting $\alpha = \kappa_1/\kappa_0$,

$$A = \frac{(\alpha-1)^2(3\alpha+5)(5\alpha+3)}{4(\alpha+1)(\alpha+3)^2(3\alpha+1)} \quad \text{(A.10)}$$

The factor A is a monotonically increasing function of α for $\alpha > 1$.

At large separations between the molecule and the domain, the size R of the domain becomes a relevant scale, and its boundary can no longer be treated as an infinite wall. In this case, the interaction can be evaluated as [62]

$$U(x) = k_B T \frac{BD_R + B_R D}{2\pi^2\kappa_0^2 x^4} = -\tilde{A} k_B T \frac{a^2 R^2}{x^4}, \quad \text{(A.11)}$$

where

$$\tilde{A} = \frac{2(\alpha-1)^2(3\alpha+5)}{(\alpha+1)(\alpha+3)^2}. \quad \text{(A.12)}$$

Note that, by taking the appropriate limits, this expression reproduces previous analytical results found in the literature [31,52].

When considering a single molecule diffusing in the vicinity of a sorting domain, one of the two regimes in Eq. (A.9) and Eq. (A.11) should be considered depending on the distance. A convenient interpolation formula for the membrane-mediated interaction energy between a molecule and a sorting domain of radius R, valid across different asymptotic regimes, is given by the simplest two-point Padé approximant [63]

$$U(r) = -k_B T \frac{R^2}{r^2}\left[\frac{Aa^2}{(r-R)^2+a^2} + (\tilde{A}-A)\frac{a^2}{r^2}\right] \quad \text{(A.13)}$$

where $r = x + R$ is the distance from the molecule to the center of the domain. This reduces to Eq. A.11 when $r \gg R$, $r \gg a$, and to Eq. A.9 in the limit $r \sim R$ and $r - R \gg a$, while also avoiding the unphysical singularity at $x = 0$.

B Simulation protocol

Simulations are performed according to a protocol that employs a Monte Carlo technique to sample Gibbs distributed configurations of the membrane, and a sub-lattice continuum Langevin equation for particle dynamics within lattice cells. Each Monte Carlo sweep (MCS) is executed as follows:

Membrane: Each site of the lattice is visited in random order, and a random displacement of the height of the surface at that site is proposed, with uniform probability within an interval of amplitude $2l_0$ centered around the previous position. The move is accepted or rejected according to the Metropolis criterion. The value of l_0 is chosen to achieve an acceptance rate of approximately 50% for the proposed moves.

Diffusion: After each membrane MCS, each lattice site i is visited in random order. If a particle is present, the auxiliary variables $x_i^{(t)}$ and $y_i^{(t)}$ are updated according to the following rule:

$$\begin{aligned} x_i^{t+1} &= x_i^t + \frac{F_x^t(x_i^t) + \sqrt{2\gamma k_B T}\,\eta^t}{\gamma} \\ y_i^{t+1} &= y_i^t + \frac{F_y^t(y_i^t) + \sqrt{2\gamma k_B T}\,\eta^t}{\gamma} \end{aligned} \tag{B.1}$$

where η^t is a Gaussian noise with zero mean and variance 1, and $F_x^t(x), F_y^t(y)$ are forces acting on the molecule along the x and y directions at time t and position (x, y). The constant γ plays the role of the friction coefficient in the Langevin equation and sets the average length of the discrete steps of the auxiliary random walk. To ensure effective sampling, it is required that $\gamma \gg |F|$. The coordinates $(x_i^{(t)}, y_i^{(t)})$ can be interpreted as the sublattice position of the molecule at site i at time t. The forces acting on the particle are evaluated as $-\nabla U$, where U is the discretized membrane energy, smoothed through a quadratic interpolation, in order to achieve sub-lattice resolution. When $x_i^t > h/2$ (respectively, $< -h/2$), molecules are moved one lattice site forward (respectively, backward) along the x direction. If the destination site is occupied, the molecules are not moved, and their position is reset to $x_i^t = h/2$ (respectively, $-h/2$). The same procedure is applied in the y direction.

The sublattice Langevin dynamics for molecules is used to accurately capture the fast-membrane-fluctuation regime. By selecting a sufficiently large value of γ, we ensure that the particle samples a large-enough number of membrane configurations before reaching the jump condition. For all the simulations performed, we set $\gamma = 500\, k_B T/h^2$.

Insertion: A site is randomly selected, and if it is empty, a particle is inserted with probability k_I. As noted in Ref. [64], the more rigid are the molecules, the lower is their diffusivity. In order to properly compare the results for $\bar{\rho}$ obtained at different κ_1/κ_0 ratios, it is important to ensure that, although k_D is different for each κ_1/κ_0, the dimensionless flux $r = \phi/k_D$ remains the same. This is accomplished by measuring the diffusion rate $k_D^{(t)}$ and the molecule density $\rho^{(t)}$ at each MCS. These values are then used to adjust the insertion rate according to the formula $k_I^{(t)} = r k_D^{(t)}/(1-\rho^{(t)})$. This procedure guarantees that the dimensionless flux mantains the assigned value r. Observe that since one MCS is taken as the time unit, the insertion probability k_I per MCS can be interpreted as an insertion rate. Similarly, the diffusion rate k_D of free molecules—those jumping between two sites lacking occupied nearest neighbors—is determined as the ratio of accepted diffusive jumps.

Extraction: if a connected component containing $\geq N_E$ occupied sites is found in the system, all particles this connected component are removed.

References

[1] M. Kaksonen and A. Roux, *Mechanisms of clathrin-mediated endocytosis*, Nat. Rev. Molec. Cell Biol. **19**, 313 (2018), doi:10.1038/nrm.2017.132.

[2] B. B. Allan and W. E. Balch, *Protein sorting by directed maturation of Golgi compartments*, Science **285**, 63 (1999), doi:10.1126/science.285.5424.63.

[3] G. Zanetti, K. B. Pahuja, S. Studer, S. Shim and R. Schekman, *COPII and the regulation of protein sorting in mammals*, Nat. Cell Biol. **14**, 20 (2012), doi:10.1038/ncb2390.

[4] J. C. Stachowiak, C. C. Hayden and D. Y. Sasaki, *Steric confinement of proteins on lipid membranes can drive curvature and tubulation.*, Proc. Natl. Acad. Sci. U.S.A. **107**, 7781 (2010), doi:10.1073/pnas.0913306107.

[5] P. Sens, L. Johannes and P. Bassereau, *Biophysical approaches to protein-induced membrane deformations in trafficking*, Curr. Op. Cell Biol. **20**, 476 (2008), doi:10.1016/j.ceb.2008.04.004.

[6] Z. Chen, E. Atefi and T. Baumgart, *Membrane shape instability induced by protein crowding.*, Biophys. J. **111**, 1823 (2016), doi:10.1016/j.bpj.2016.09.039.

[7] L. Foret and P. Sens, *Kinetic regulation of coated vesicle secretion*, Proc. Natl. Acad. Sci. U.S.A. **105**, 14763 (2008), doi:10.1073 / pnas.0801173105.

[8] I. Mellman and W. J. Nelson, *Coordinated protein sorting, targeting and distribution in polarized cells.*, Nat. Rev. Mol. Cell Biol. **9**, 833 (2008), doi:10.1038/nrm2525.

[9] S. Staubach and F.-G. Hanisch, *Lipid rafts: signaling and sorting platforms of cells and their roles in cancer*, Expert Rev. Proteom. **8**, 263 (2011), doi:10.1586/epr.11.2.

[10] O. Pornillos, J. E. Garrus and W. I. Sundquist, *Mechanisms of enveloped RNA virus budding*, Trends Cell Biol. **12**, 569 (2002), doi:10.1016/S0962-8924(02)02402-9.

[11] J. S. Rossman and R. A. Lamb, *Influenza virus assembly and budding*, Virology **411**, 229 (2011), doi:10.1016/j.virol.2010.12.003.

[12] P. Sengupta and J. Lippincott-Schwartz, *Revisiting membrane microdomains and phase separation: a viral perspective*, Viruses **12**, 745 (2020), doi:10.3390/v12070745.

[13] B. B. Motsa and R. V. Stahelin, *Lipid–protein interactions in virus assembly and budding from the host cell plasma membrane*, Bioch. Soc. Trans. **49**(4), 1633 (2021), doi:10.1042/BST20200854.

[14] M. Zamparo, D. Valdembri, G. Serini, I. V. Kolokolov, V. V. Lebedev, L. Dall'Asta and A. Gamba, *Optimality in self-organized molecular sorting*, Phys. Rev. Lett. **126**, 088101 (2021), doi:10.1103/PhysRevLett.126.088101.

[15] E. Floris, A. Piras, F. S. Pezzicoli, M. Zamparo, L. Dall'Asta and A. Gamba, *Phase separation and critical size in molecular sorting*, Phys. Rev. E **106**, 044412 (2022), doi:10.1103/PhysRevE.106.044412.

[16] A. Piras, E. Floris, L. Dall'Asta and A. Gamba, *Sorting of multiple molecular species on cell membranes*, Phys. Rev. E **108**, 024401 (2023), doi:10.1103/PhysRevE.108.024401.

[17] K. J. Day, G. Kago, L. Wang, J. B. Richter, C. C. Hayden, E. M. Lafer and J. C. Stachowiak, *Liquid-like protein interactions catalyse assembly of endocytic vesicles*, Nat. Cell Biol. **23**, 366 (2021), doi:10.1038/s41556-021-00646-5.

[18] X. Wang, Z. Chen, M. Mettlen, J. Noh, S. L. Schmid and G. Danuser, *DASC, a sensitive classifier for measuring discrete early stages in clathrin-mediated endocytosis*, Elife **9**, e53686 (2020), doi:10.7554/elife.53686.

[19] A. A. Hyman, C. A. Weber and F. Jülicher, *Liquid-liquid phase separation in biology*, Ann. Rev. Cell and Dev. Biol. **30**, 39 (2014), doi:10.1146/annurev-cellbio-100913-013325.

[20] Y. Shin and C. P. Brangwynne, *Liquid phase condensation in cell physiology and disease*, Science **357**, eaaf4382 (2017), doi:10.1126/science.aaf4382.

[21] E. Floris, A. Piras, L. Dall'Asta, A. Gamba, E. Hirsch and C. C. Campa, *Physics of compartmentalization: How phase separation and signaling shape membrane and organelle identity*, Comp. Struct. Biotech. J. **19**, 3225 (2021), doi:10.1016/j.csbj.2021.05.029.

[22] T. S. Harmon, A. S. Holehouse, M. K. Rosen and R. V. Pappu, *Intrinsically disordered linkers determine the interplay between phase separation and gelation in multivalent proteins*, eLife **6**, e30294 (2017), doi:10.7554/eLife.30294.

[23] A. Gamba, A. De Candia, S. Di Talia, A. Coniglio, F. Bussolino and G. Serini, *Diffusion-limited phase separation in eukaryotic chemotaxis*, Proc. Natl. Acad. Sci. U.S.A. **102**(47), 16927 (2005), doi:10.1073/pnas.0503974102.

[24] A. Gamba, I. Kolokolov, V. Lebedev and G. Ortenzi, *Patch coalescence as a mechanism for eukaryotic directional sensing*, Phys. Rev. Lett. **99**, 158101 (2007), doi:10.1103/PhysRevLett.99.158101.

[25] J. Halatek, F. Brauns and E. Frey, *Self-organization principles of intracellular pattern formation*, Phil. Trans. R. Soc. B **373**, 20170107 (2018), doi:10.1098/rstb.2017.0107.

[26] F. Brauns, J. Halatek and E. Frey, *Phase-space geometry of mass-conserving reaction-diffusion dynamics*, Phys. Rev. X **10**, 041036 (2020), doi:10.1103/PhysRevX.10.041036.

[27] C. A. Weber, D. Zwicker, F. Jülicher and C. F. Lee, *Physics of active emulsions*, Rep. Progr. Phys. **82**(6), 064601 (2019), doi:10.1088/1361-6633/ab052b.

[28] S. Saha, A. Das, C. Patra, A. A. Anilkumar, P. Sil, S. Mayor and M. Rao, *Active emulsions in living cell membranes driven by contractile stresses and transbilayer coupling.*, Proc. Natl. Acad. Sci. U.S.A. **119**, e2123056119 (2022), doi:10.1073/pnas.2123056119.

[29] M. Zamparo, F. Chianale, C. Tebaldi, M. Cosentino-Lagomarsino, M. Nicodemi and A. Gamba, *Dynamic membrane patterning, signal localization and polarity in living cells*, Soft Matter **11**, 838 (2015), doi:10.1039/C4SM02157F.

[30] S. N. Weber, C. A. Weber and E. Frey, *Binary mixtures of particles with different diffusivities demix*, Phys. Rev. Lett. **116**, 058301 (2016), doi:10.1103/PhysRevLett.116.058301.

[31] M. Goulian, R. Bruinsma and P. Pincus, *Long-range forces in heterogeneous fluid membranes*, Europh. Lett. **22**, 145 (1993), doi:10.1209/0295-5075/22/2/012.

[32] T. R. Weikl, *Membrane-mediated cooperativity of proteins*, Ann. Rev. Phys. Chem. **69**, 521 (2018), doi:10.1146/annurev-physchem-052516-050637.

[33] A. J. Jin, K. Prasad, P. D. Smith, E. M. Lafer and R. Nossal, *Measuring the elasticity of clathrin-coated vesicles via atomic force microscopy*, Bioph. J. **90**, 3333 (2006), doi:10.1529/biophysj.105.068742.

[34] A. Zemel, A. Ben-Shaul and S. May, *Modulation of the spontaneous curvature and bending rigidity of lipid membranes by interfacially adsorbed amphipathic peptides*, J. Phys. Chem. B **112**, 6988 (2008), doi:10.1021/jp711107y.

[35] J. D. Nickels, X. Cheng, B. Mostofian, C. Stanley, B. Lindner, F. A. Heberle, S. Perticaroli, M. Feygenson, T. Egami, R. F. Standaert *et al.*, *Mechanical properties of nanoscopic lipid domains*, J. Am. Chem. Soc. **137**, 15772 (2015), doi:10.1021/jacs.5b08894.

[36] I. M. Lifshitz and V. V. Slezov, *Kinetics of diffusive decomposition of supersaturated solid solutions*, Sov. Phys. JETP **35**, 331 (1959).

[37] V. V. Slezov, *Kinetics of First-Order Phase Transitions*, Wiley-VCH, ISBN 9783527627769, doi:10.1002/9783527627769 (2009).

[38] P. Canham, *The minimum energy of bending as a possible explanation of the biconcave shape of the human red blood cell*, J. Theor. Biol. **26**, 61 (1970), doi:10.1016/S0022-5193(70)80032-7.

[39] W. Helfrich, *Elastic properties of lipid bilayers: Theory and possible experiments*, Z. Naturforsch. C **28**, 693 (1973), doi:doi:10.1515/znc-1973-11-1209.

[40] L. D. Landau and E. M. Lifshitz, *Theory of elasticity*, vol. 7 of *Course of Theoretical Physics*, Butterworth-Heinemann (1986).

[41] M. Hu, J. J. Briguglio and M. Deserno, *Determining the gaussian curvature modulus of lipid membranes in simulations*, Bioph. J. **102**, 1403 (2012), doi:10.1016/j.bpj.2012.02.013.

[42] M. Deserno, K. Kremer, H. Paulsen, C. Peter and F. Schmid, *Computational Studies of Biomembrane Systems: Theoretical Considerations, Simulation Models, and Applications*, pp. 237–283, ISBN 9783319058283, doi:10.1007/12_2013_258 (2013).

[43] H. Noguchi, *Virtual bending method to calculate bending rigidity, saddle-splay modulus, and spontaneous curvature of thin fluid membranes*, Phys. Rev. E **102**(5), 053315 (2020), doi:10.1103/physreve.102.053315.

[44] F. Brochard-Wyart and J. Lennon, *Frequency spectrum of flicker phenomenon in erythrocytes.*, J. Phys. **36**, 1035 (1975), doi:10.1051/jphys:0197500360110103500.

[45] S. Ramadurai, A. Holt, V. Krasnikov, G. van den Bogaart, J. A. Killian and B. Poolman, *Lateral diffusion of membrane proteins*, J. Am. Chem. Soc. **131**(35), 12650 (2009), doi:10.1021/ja902853g.

[46] K. Weiß, A. Neef, Q. Van, S. Kramer, I. Gregor and J. Enderlein, *Quantifying the diffusion of membrane proteins and peptides in black lipid membranes with 2-focus fluorescence correlation spectroscopy*, Biophys. J. **105**, 455 (2013), doi:10.1016/j.bpj.2013.06.004.

[47] A. Naji and F. L. Brown, *Diffusion on ruffled membrane surfaces*, J. Chem. Phys. **126**, 06B611 (2007), doi:10.1063/1.2739526.

[48] F. Divet, T. Biben, I. Cantat, A. Stephanou, B. Fourcade and C. Misbah, *Fluctuations of a membrane interacting with a diffusion field*, Europh. Lett. **60**, 795 (2002), doi:10.1209/epl/i2002-00378-5.

[49] M. Goulian, R. Bruinsma and P. Pincus, *Long-range forces in heterogeneous fluid membranes - erratum*, Europh. Lett. **23**, 155 (1993), doi:10.1209/0295-5075/23/2/014.

[50] J.-M. Park and T. C. Lubensky, *Interactions between membrane inclusions on fluctuating membranes*, J. Phys. I **6**, 1217 (1996), doi:10.1051/jp1:1996125.

[51] A.-F. Bitbol, P. G. Dommersnes and J.-B. Fournier, *Fluctuations of the Casimir-like force between two membrane inclusions*, Phys. Rev. E **81**, 050903 (2010), doi:10.1103/PhysRevE.81.050903.

[52] H.-K. Lin, R. Zandi, U. Mohideen and L. P. Pryadko, *Fluctuation-induced forces between inclusions in a fluid membrane under tension*, Phys. Rev. Lett. **107**, 228104 (2011), doi:10.1103/physrevlett.107.228104.

[53] C. Yolcu and M. Deserno, *Membrane-mediated interactions between rigid inclusions: an effective field theory*, Phys. Rev. E **86**, 031906 (2012), doi:10.1103/PhysRevE.86.031906.

[54] E. Reister and U. Seifert, *Lateral diffusion of a protein on a fluctuating membrane*, Europh. Lett. **71**, 859 (2005), doi:10.1209/epl/i2005-10139-6.

[55] E. Reister-Gottfried, S. M. Leitenberger and U. Seifert, *Diffusing proteins on a fluctuating membrane: Analytical theory and simulations*, Phys. Rev. E **81**, 031903 (2010), doi:10.1103/PhysRevE.81.031903.

[56] T. R. Weikl, *Dynamic phase separation of fluid membranes with rigid inclusions*, Phys. Rev. E **66**, 061915 (2002), doi:10.1103/PhysRevE.66.061915.

[57] Y. Park, C. A. Best, K. Badizadegan, R. R. Dasari, M. S. Feld, T. Kuriabova, M. L. Henle, A. J. Levine and G. Popescu, *Measurement of red blood cell mechanics during morphological changes*, Proc. Natl. Acad. Sci. U.S.A. **107**, 6731 (2010), doi:10.1073/pnas.0909533107.

[58] W. Rawicz, K. C. Olbrich, T. McIntosh, D. Needham and E. Evans, *Effect of chain length and unsaturation on elasticity of lipid bilayers*, Bioph. J. **79**, 328 (2000), doi:10.1016/s0006-3495(00)76295-3.

[59] M. Zamparo, L. Dall'Asta and A. Gamba, *On the mean residence time in stochastic lattice-gas models*, J. Stat. Phys. **174**, 120 (2019), doi:10.1007/s10955-018-2175-x.

[60] R. Phillips, T. Ursell, P. Wiggins and P. Sens, *Emerging roles for lipids in shaping membrane-protein function*, Nature **459**, 379 (2009), doi:10.1038/nature08147.

[61] D. Nelson, T. Piran and S. Weinberg, *Statistical Mechanics of Membranes and Surfaces*, World Scientific, 2nd edn., doi:10.1142/5473 (2004).

[62] E. Pikina, A. Muratov, E. Kats and V. Lebedev, *Long-range interactions between membrane inclusions: Electric field induced giant amplification of the pairwise potential*, Ann. Phys. (N.Y.) **447**, 168916 (2022), doi:https://doi.org/10.1016/j.aop.2022.168916.

[63] A. George Jr, J. L. Gammel *et al.*, *The Padé approximant in theoretical physics*, Academic Press (1971).

[64] A. Naji, P. J. Atzberger and F. L. Brown, *Hybrid elastic and discrete-particle approach to biomembrane dynamics with application to the mobility of curved integral membrane proteins*, Phys. Rev. Lett. **102**, 138102 (2009), doi:10.1103/PhysRevLett.102.138102.